J. Ind. Geophys. Union (November 2017)
v.21, no.6, pp: 490-499

Study of Effects of Basin Shape, Shape-Ratio and Angle of Incidence of SH-Wave on Ground Motion Characteristics and Aggravation Factors

Kamal*[1] and Komal Rani[2]

[1]Department of Geophysics, Kurukshetra University Kurukshetra, Haryana
[2]B.A.R. Janta College, Kaul, Kaithal, Haryana
*Corresponding Author: kamalbattan@gmail.com

ABSTRACT

This paper presents the effects of basin-shape, shape-ratio, impedance contrast (IC), sediment-damping and angle of incidence of SH-waves on the ground motion characteristics and associated spatial variations of average spectral amplification (ASA) and average aggravation factor (AAF) in the basins. Seismic responses of basin models were simulated using a SH wave fourth-order spatial accurate time-domain finite-difference algorithm based on staggered-grid approximation of viscoelastic velocity-stress wave equations. The obtained ASA and AAF were largest in the semi-circular basin and least in the trapezoidal basin for the considered model parameters. On an average, an increase of ASA and AAF were obtained with an increase of IC, sediment quality factor and the basin shape-ratio (in the shape-ratio range 0.03 - 0.16). An increase of ASA and AAF with the increase of angle of incidence of SH-wave was inferred.

Key words: Basin effects, basin-generated Love waves, aggravation factor and finite difference simulation.

INTRODUCTION

Seismic microzonation of an area is very much essential for the minimization of the impact of the earthquake hazard and prediction of seismic risk as well as developing cost effective earthquake resistant design of structures. A highly variable damage patterns have been reported in a particular basin due to the physical phenomenon like double-resonance (Dobry and Vacetic, 1987; Narayan et al., 2002), basin generated surface waves (Bard and Bouchon, 1980; Kawase, 1996; Hatyama et al., 1995; Pitarka et al., 1998; Graves et al., 1998; Narayan 2005; Narayan and Singh, 2006; Kamal and Narayan, 2014; 2015), basement focusing effects (Gao et al., 1996; Booth et al., 2004; Narayan and Kumar, 2013; 2014) and site effects and attenuation characteristics (Joshi et al., 2012; Kumar et al., 2013; 2014; 2015; Kumar et al., 2016) etc. Basin generated surface waves were confirmed based on the recorded ground motion in the Santa Monica and Kobe basins, theoretical studies and the observed damages during the 1994 Northridge earthquake and 1995 Kobe, Japan earthquake (Kawase, 1996; Graves et al., 1998; Pitarka et al., 1998). There are other numerous consistent macro-seismic observations showing a significant increase in damage severity in narrow zones located near the basin-edge (Poceski, 1969; Yuan and Huang, 1992). A significant number of scientists have studied the effects of soil layering on the characteristics of edge generated surface waves (Semblat et al., 2005; Narayan and Singh, 2006). Bard and Bouchon (1980) reported preferential surface wave generation in case of larger angle of incidence of body wave at the basin edge.

The current practice of seismic microzonation in many countries is to transfer the bedrock motion to the surface using the 1D SH-wave response of a soil column. Based on the theoretical studies, it was inferred that the 1D response was inadequate to explain the observed damages in Santa Monica during the 1994 Northridge earthquake (Graves et al., 1998) and in Kobe basin during the 1995 Kobe, Japan earthquake (Pitarka et al., 1998). To incorporate the 2D/3D complex site effects in seismic microzonation, Chavez-Garcia and Faccioli (2000) have proposed the term aggravation factor (aggravation factor is simply the extra spectral amplification due to the complex 2D/3D site effects over the 1D response of the soil column). In the basins, as mentioned above, an important cause for the spatial variation of the seismic ground motions is the basin generated surface wave.

In this paper, a detailed study of effects of basin-shape, shape-ratio, impedance contrast (IC), sediment-damping and angle of incidence of SH-waves on the ground motion characteristics and associated spatial variations of average spectral amplification (ASA) and average aggravation factor (AAF) in the basins are documented. Seismic responses of basin models were simulated using a SH wave fourth-order spatial accurate time-domain finite-difference (FD) algorithm based on staggered-grid approximation of viscoelastic velocity-stress wave equations. Snapshots have also been computed for inferring the development

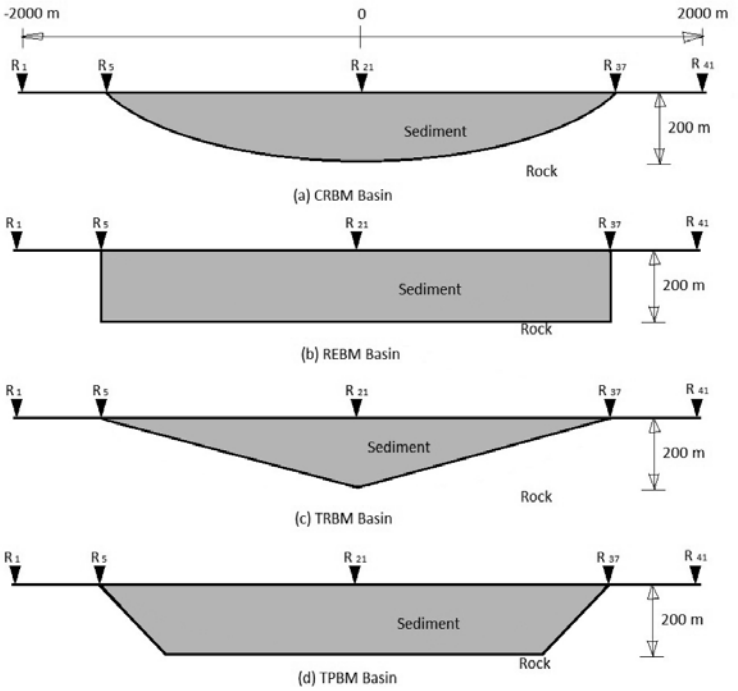

Figure 1a-d. shows the considered semi-circular (CRBM), rectangular (REBM), triangular (TRBM) and trapezoidal (TPBM) basin models, respectively.

Table 1. The velocities and quality factors, density and unrelaxed moduli for the sediment and rock.

Model	Vs (m/s)	Density (g/cc)	Q_S	Unrelaxed Moduli (GPa)
Sediment	650	2.00	65	0.8707
Rock	2000	2.40	200	9.6938

of basin generated surface waves and their back and forth propagation in the basin.

Salient Features of the Used SH Wave FD Program

A computer program developed by Narayan and Kumar (2013),which is based on the staggered grid (2,4) finite-difference approximation of the viscoelastic SH wave equation for the heterogeneous anelastic medium is used. The frequency-dependent damping in the time-domain FD simulations is incorporated based on the GMB-EK rheological model (Emmerich and Korn, 1987; Kristek and Moczo, 2003). A material independent anelastic function developed by Kristek and Moczo (2003) was used since it is preferable in case of material discontinuities in the FD grid (Narayan and Kumar, 2013; 2014). Both the sponge boundary (Israeli and Orszag, 1981) and A1 absorbing boundary (Clayton and Engquist, 1977) conditions were implemented on the model edges to avoid the edge reflections (Kumar and Narayan, 2008). In order to avoid the thickness discrepancy of the first sediment layer, which causes an increase of value of the numerically computed fundamental frequency, VGR-stress imaging technique proposed by Narayan and Kumar (2008) is used.

Effects of Basin Shape

To study the effects of shape of basin on the ground motion characteristics, four basin models, namely, semi-circular (CRBM), rectangular (REBM), triangular (TRBM) and trapezoidal (TPBM) basins have been considered. The remaining geometrical parameters like width, maximum depth of sediment and inelastic parameters of the sediment and rock are the same for all the four considered basin models. The north-south cross sections of the CRBM, REBM, TRBM and TPBM basin models are shown in figure 1a-d, respectively. The width and maximum depth of all the basins are 3000 m and 200 m, respectively. All the distances are measured with respect to the centre of basins. A horizontal plane wave front has been generated at a depth of 300 m using various point sources. The point source has been generated in the form of Ricker wavelet. The dominant frequency in the considered Ricker wavelet was 4.0 Hz and frequency bandwidth 0-10 Hz. Seismic responses have been computed at 41 equidistant (100 m

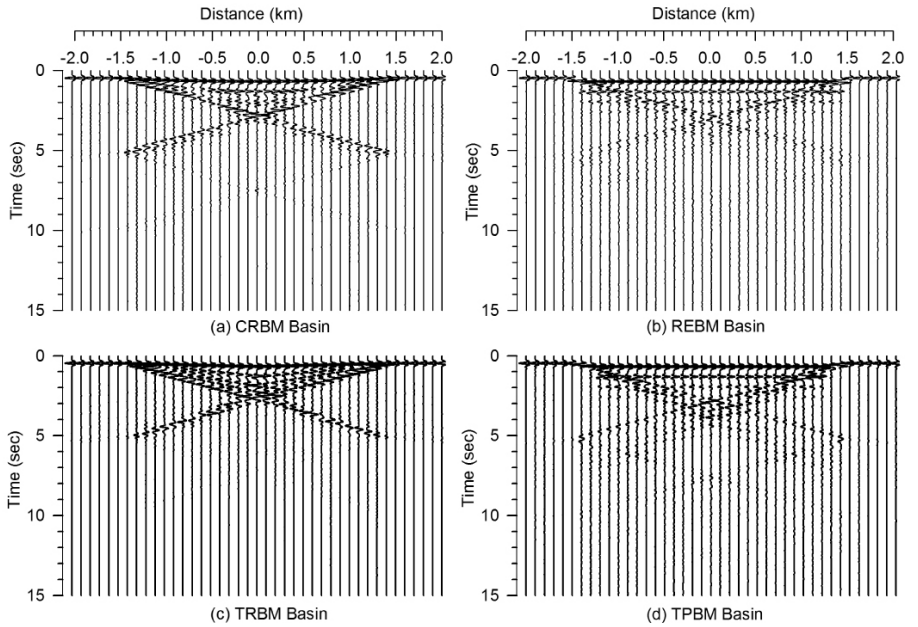

Figure 2a-d. The seismic responses of the CRBM, REBM, TRBM and TPBM basins, respectively.

apart) receiver points, extending 2000 m south to 2000 m north of centre of the basins. The velocities and quality factors for the P- and S-waves at a reference frequency 1.0 Hz (Fr=1.0 Hz), density and unrelaxed moduli μ (modulus of rigidity), K (bulk modulus), and λ (Lame's parameter) for the sediment and rock are given in table 1. Four relaxation frequencies as 0.02 Hz, 0.2 Hz, 2.0 Hz and 20.0 Hz were used for the computations of the unrelaxed moduli. To reduce the requirement of computational time and memory, the basin models have been discretized with a continuous variable grid size (Narayan and Kumar, 2008). The vertical grid size was 5 m from free surface to a depth of 265 m and 15 m thereafter. Similarly, in the horizontal direction, the grid size is 5 m from 2100 m south to 2100 m north of centre of basins and 15 m thereafter. The time step is chosen to be 0.001 second to avoid stability problem. The seismic response of the model with no sediment is also computed for the quantification of spectral amplifications.

Figure 2a-d shows the seismic responses of CRBM, REBM, TRBM and TPBM basin models, respectively. The incident SH-wave, its multiple and basin-generated Love waves and multiples of the basin-generated Love waves are the first, second, third and fourth arrivals in a chronological order. Based on the analysis of figure 2, the fundamental and first modes of Love waves can be inferred in the basins. But, their characteristics are highly variable with basin-shape. Very large amplitude at the centre of basin may be due to the constructive interference of the Love waves generated at the left and right edges of the basin. A leakage of the Love wave energy in the rock can be inferred at each reflection of Love waves at the basin-edge. Further, it appears that the Love waves are highly dispersive in nature depending on the basin-shape. The basin generated Love waves can be inferred in all the basins but their characteristics are highly variable from basin to basin. So, it may be concluded that basin-shape plays an important role in amplification of incident SH-waves and the basin generated Love waves.

Snapshots

In order to further infer the development of Love waves in the basins, snapshots in a rectangular area in the CRBM basin have been computed at different moments. Snapshots were computed in a rectangular area extending 2000 m south to 2000 m north of centre of basin and from free surface to a depth of 360 m. Figures 3 shows the snapshots at different times. The snapshots at times 0.45s to 1.35s depict that the incident plane wave front of SH-wave, it's multiple and generation and propagation of Love waves towards the centre of basin. Similarly, snapshots at times 1.65s to 3.45s depict the propagation of Love waves in the basin.

Average spectral amplification

The spectral amplifications were computed just by taking the ratio of spectra of responses with and without basin in the model. The spectral ratio has been used to compute the average spectral amplification (ASA) at a particular location. Figure 4a illustrates the comparison of spatial variation of ASA in different basins. An analysis of this figure reveals that the largest and lowest ASA are obtained in the CRBM and TPBM basins, respectively. Further,

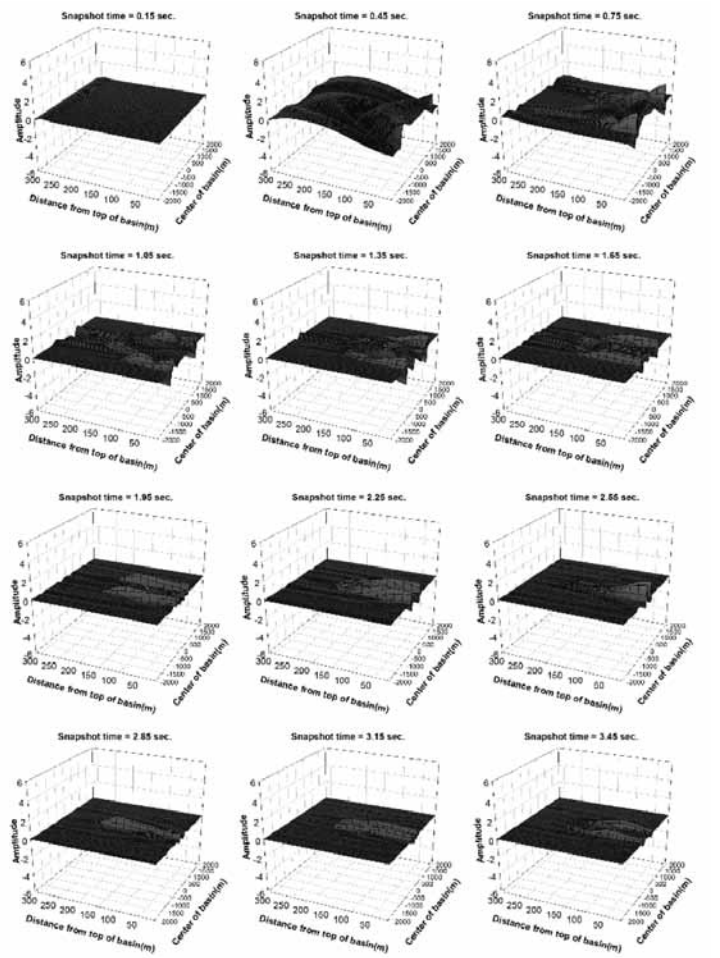

Figure 3. Snapshots of response of the CRBM basin at different moments.

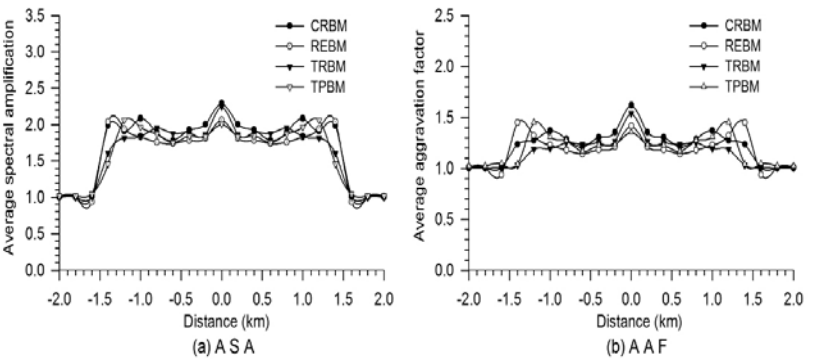

Figure 4a-b. Spatial variation of ASA and AAF, respectively in the CRBM, REBM, TRBM and TPBM basins.

largest ASA in the CRBM and TRBM basins are occurring at the centre of basin.

Average aggravation factor

In order to study the effects of shape of basins on the spatial variation of average aggravation factor (AAF), spectral aggravation factors were computed just by taking the spectral ratio of 2D response with the 1D response of the model at a particular location. Then spectral aggravation factors were used to find out the AAF at different locations in the basins. Figure 4b shows the comparison of spatial variation of AAF caused by mainly Love waves. Analysis of this figure depicts that the trends of spatial variation of AAF is almost the same

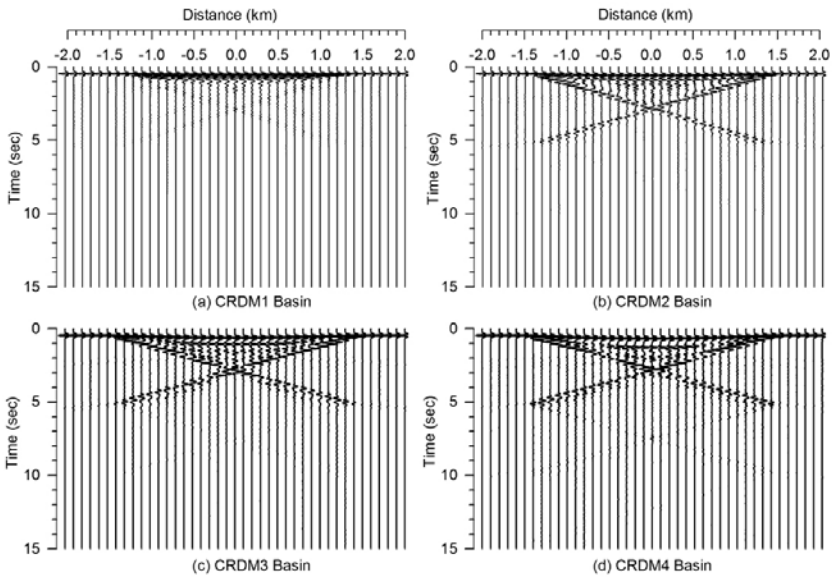

Figure 5. The seismic responses of the CRDM1-CRDM4 basins, respectively.

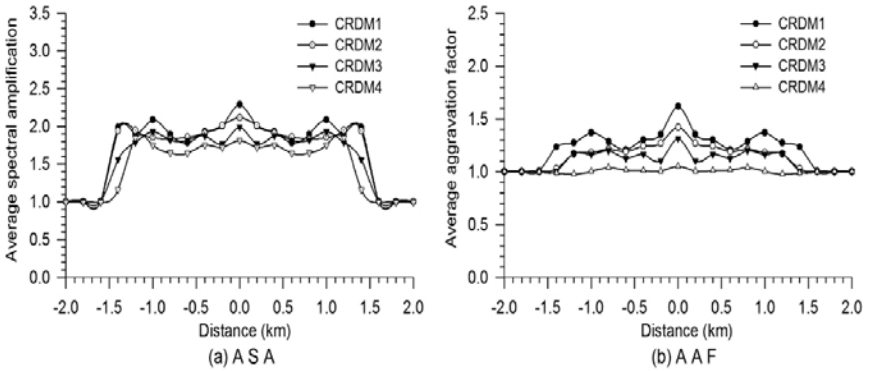

Figure 6. Spatial variations of ASA and AAF, respectively in the CRDM-CRDM4 basins.

as that of the ASA in different basins. The largest AAF of the order of 1.6 was obtained at the centre of the CRBM basin. The cause of increase of AAF towards the centre of basins may be the constructive interference of the surface waves moving from opposite direction. So, it can be inferred that very large damage may occur in the central part of the basins, particularly TRBM and CRBM basins.

Effects of Shape Ratio of Basin

The shape-ratio of basin is defined as the ratio of maximum depth of basin with the half-width of basin. The shape-ratio of basin has been changed by changing the depth as well as width of the basin. The effects of shape-ratio for both the cases have been studied. First, seismic responses of four basin CRDM1-CRDM4 models with maximum depth of sediment as 200 m, 150 m, 100 m and 50 m and a fixed width as 3000 m with shape-ratios as 0.13, 0.10, 0.06 and 0.03, respectively have been computed. The seismic responses of another four basin CRWM1-CRWM4 models with width as 3500 m, 3000 m, 2500 m and 2000 m and a fixed maximum depth as 200 m with shape-ratios as 0.11, 0.13, 0.16 and 0.20, respectively have also been computed. So, finally the range of basin-shape-ratio is 0.03-0.2. Figure 5a-d shows the seismic responses of the CRDM1-CRDM4 models, respectively. The characteristics of the SH-wave multiples and the basin generated surface waves are highly variable with the change of shape-ratio. A comparison of spatial variations of ASA and AAF in the CRMD1-CRDM4 basins are given in figure 6. On an average an increase of ASA/AAF with an increase of shape-ratio can be inferred for the considered model parameters and frequency bandwidth. Similarly, Figure 7a-d shows the seismic responses of the CRDM1-CRDM4 models, respectively. The characteristics of the SH-wave multiples and the basin generated surface waves are highly variable with the change of shape-ratio. Similarly, a comparison of spatial variation of ASA and AAF in the CRWD1-CRWM4 basins are given in figure 8.

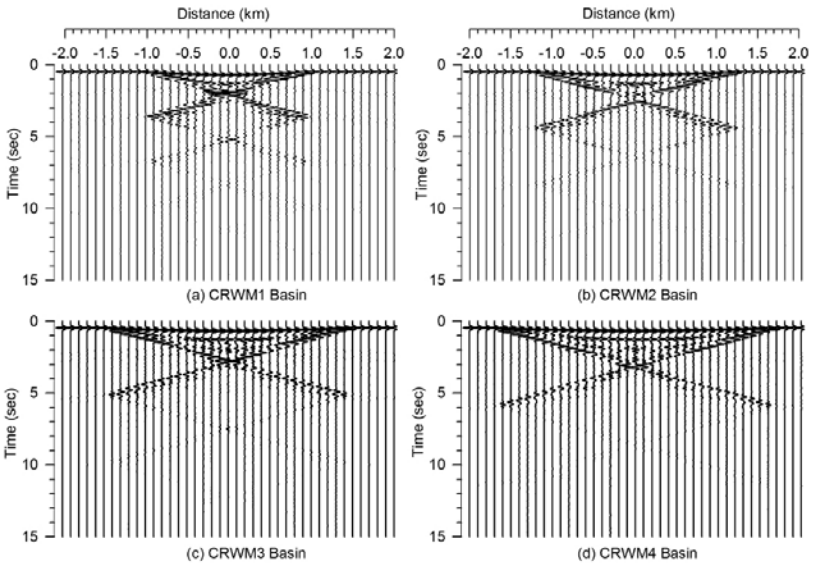

Figure 7. The seismic responses of the CRWM1-CRWM4 basins, respectively.

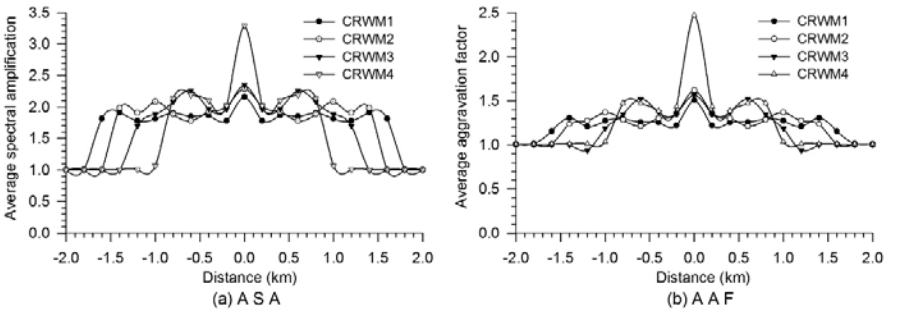

Figure 8. Spatial variations of ASA and AAF, respectively in the CRWM1-CRWM4 basins.

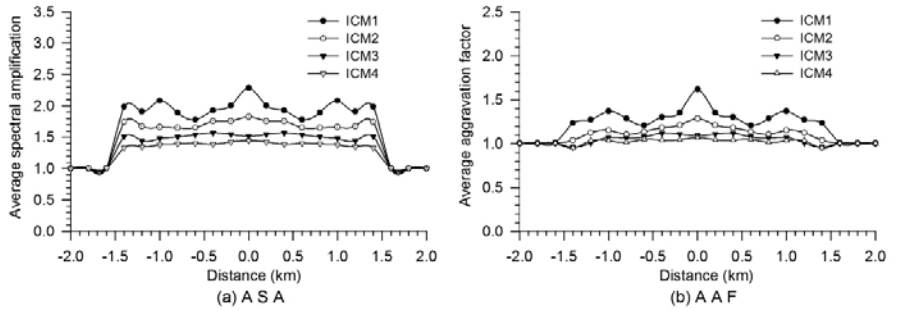

Figure 9. Spatial variations of ASA and AAF, respectively in the ICM1-ICM4 basins.

On an average an increase of ASA/AAF with an increase of shape-ratio can be inferred. So, it may be concluded that AAF/ASA increases with the increase of shape-ratio of basin, if shape-ratio is less than 0.20.

Effects of Impedance Contrast and Sediment-Damping

In this sub-section, the effects of impedance contrast (IC) and sediment-damping on the ground motion characteristics in the basin are documented. In order to find out the effects of IC on the AAF, seismic responses of 1D basin models at different locations in the basin were also computed for different IC and sediment-damping. The velocities and quality factors at reference frequency, density and un-relaxed moduli for the different ICM1-ICM4 basin models are given in table 2. The width and maximum depth of the semi-circular ICM1-ICM4 basins were taken as 3000 m and 200 m, respectively. Figure 9a-b shows the spatial variation of ASA and AAF. An increase of ASA

Table 2. The velocities and quality factors, density, IC and unrelaxed moduli for the ICM1-ICM4 basin models.

Model	Vs (m/s)	Density (g/cc)	IC	Q_S	Unrelaxed Moduli (GPa)
ICM1	650	2.00	3.69	65	0.8707
ICM2	800	2.05	2.92	80	1.3443
ICM3	950	2.10	2.40	95	1.9345
ICM4	1100	2.15	2.02	110	2.6479
Rock	2000	2.40	---	200	9.6938

Table 3. The quality factors and unrelaxed moduli for the BDM1-BDM4 basin models.

Parameters	BDM1	BDM2	BDM3	BDM4
Q_S	32.50	48.75	65.00	81.25
Unrelaxed Moduli	0.8974	0.8795	0.8707	0.8655

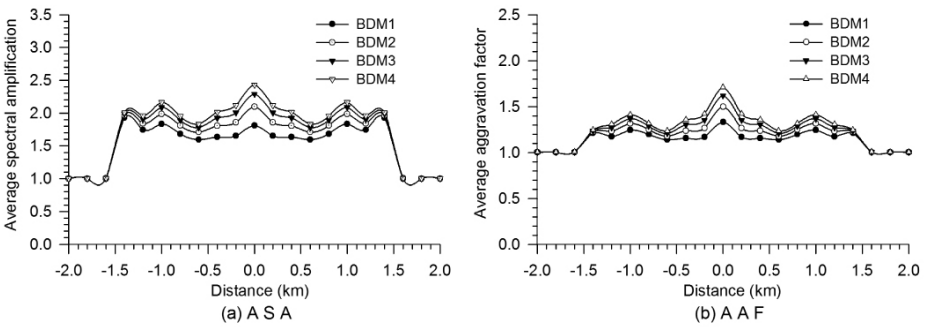

Figure 10. Spatial variations of ASA and AAF, respectively in the BDM1-BDM4 basins.

and AAF with an increase of IC can be inferred. Further, the ups and downs are increasing with an increase of IC due to the development of more and more low frequency surface waves. The interference of these lower frequency surfaces is responsible for the large ASA/AAF at the centre of basin with a large IC.

To study the effects of sediment-damping on the ground motion characteristics, seismic responses of four semi-circular BDM1-BDM4 basin models were computed for different-sediment damping. The velocities at reference frequency and density are the same as given in table 1. The quality factors at reference frequency and unrelaxed moduli for the different BDM1-BDM4 basin models are given in table 3. The width and maximum depth of the semi-circular BDM1-BDM4 basins were also taken as 3000 m and 200 m, respectively. Figure 10a-b shows the spatial variation of ASA and AAF. An increase of ASA and AAF with an increase of quality factor can be inferred. The larger increase of AAF towards the centre of basin as compared to near the basin-edge with increase of quality factor, reflects the effects of sediment-damping on the basin-generated Love waves.

Effects of Angle of Incidence of SH-Wave

To quantify the effects of angle of incidence of SH-waves on ground motion characteristics in the basin, seismic responses of the ICM1 basin model have also been computed for 20^0, 45^0 and 60^0 angles of incidence of SH-waves. The angles of incidence of SH-wave in CRAM2, CRAM3 and CRAM4 models are 20^0, 45^0 and 60^0, respectively (Figure 11). The remaining parameters for the CRAM2, CRAM3 and CRAM4 models are same. The CRAM1 model corresponds to the ICM1 model where angle of incidence of SH-wave is 0^0. Figure 12a&b show the seismic responses of the CRAM2 basin model without and with basin in model, respectively. Similarly, figures 12c&d and 12e&f show the seismic responses of the CRAM3 and CRAM4 basin model without and with basin in model, respectively. An analysis of figure 12a reflects that the inclined linear wave source (20^0) has generated SH-wave. Further, these waves have generated Love waves in the basin. Similarly, an analysis of figure 11c reflects the inclined linear SH-wave source (45^0) generation. Because of large angle of incidence of SH-wave, it appears

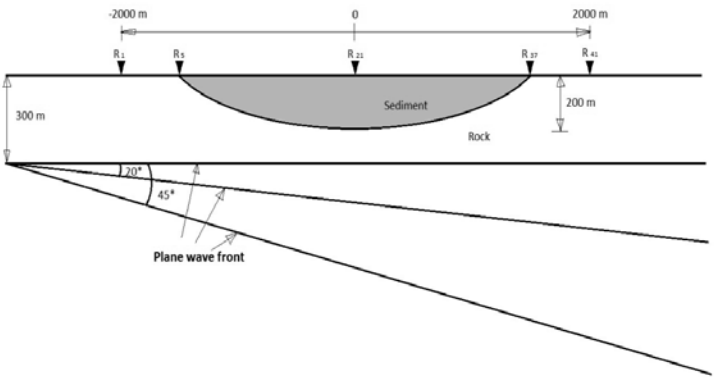

Figure 11. CRBM basin model and the incident plane wave fronts with different angle of incidence at the free surface.

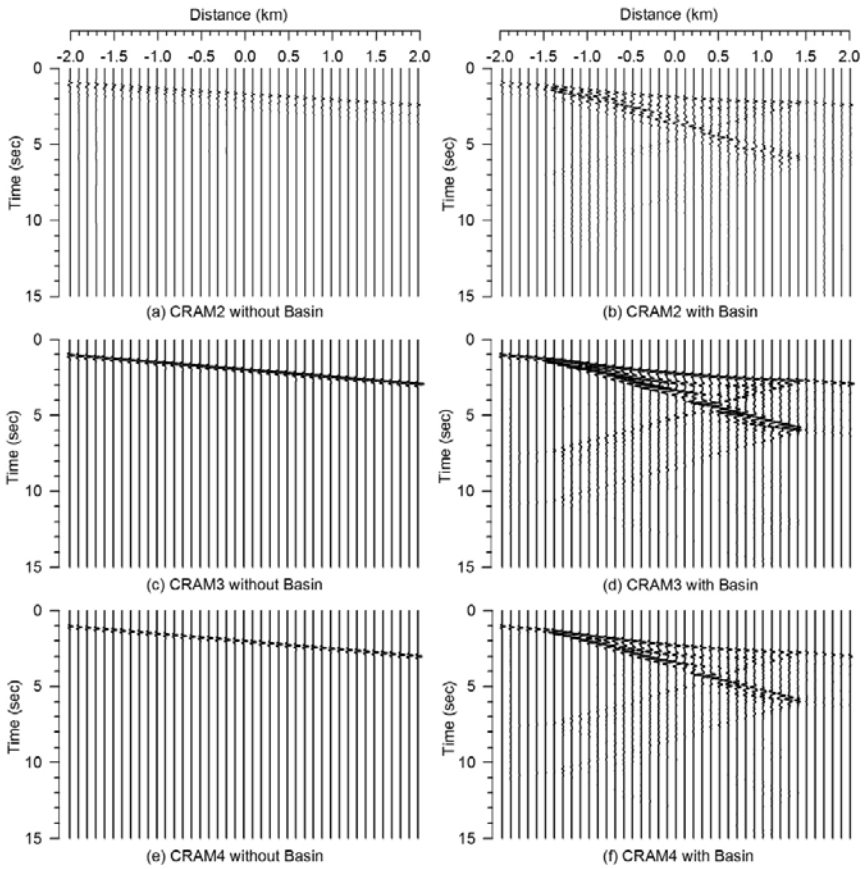

Figure 12a-f. The seismic responses of the CRAM2, CRAM3 and CRAM4 models without and with basins, respectively.

that the SH-wave has also caused Love wave at the point where the SH-wave front interacted with the free surface with considerable amplitude. An increase of amplitude of basin-generated love wave in basin can be inferred. This was also observed by Narayan (2012) and Narayan and Kumar (2013). Further, incident SH-wave has generated Love waves in the basin. So, in the CRAM3 and CRAM4 basin models, we have both the basin-generated and basin-induced Love waves (Figure 12d & 12f). A complex mode conversion of basin induced Love wave at the basin edge can also be inferred (Narayan, 2012).

Figure 13a-b depicts the comparison of spatial variations of ASA and AAF for the CRAM1-CRAM4 basin models, respectively. Analysis of figure 13 depicts that in case of angle of incidence as 20^0, 45^0 and 60^0, the amplification is largest towards the left edge of basin, in case of CRAM3 and CRAM4 models. On the other hand, the amplification is symmetrical around the centre of the

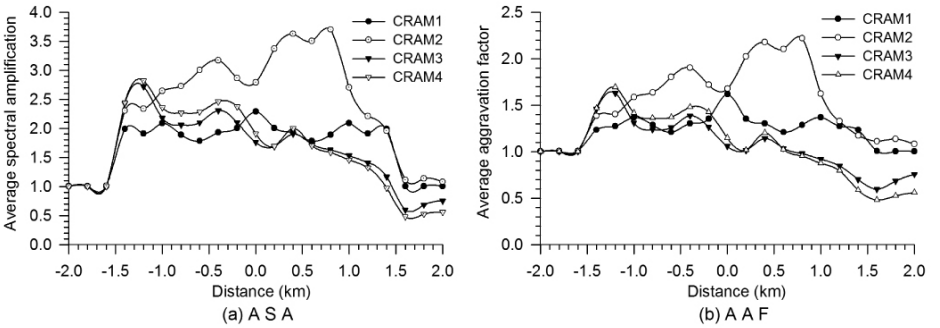

Figure 13. Spatial variations of ASA and AAF, respectively in the CRAM1-CRAM4 basins.

basin in CRAM1/ICM1 basin model. This is due to the normal incidence of the SH-waves. It can also be inferred that the level of AAF is larger in CRAM2, CRAM3 and CRAM4 models as compared to the CRAM1/ICM1 model. Further, the level of AAF is larger in CRAM4 model as compared to the CRAM3 model. So, it may be concluded that amplification of ground motion increases with the increase of angle of incidence of SH-waves.

CONCLUSIONS

Based on the analysis of seismic responses of various basin models and the computed snapshots, it is inferred that the incident SH-wave generates Love wave in the basin. The analysis of simulated responses of basins having different shapes revealed that the ground motion in the basin is highly dependent not only on the shape of basin but also on the width and largest depth of basin, while other parameters are the same. Almost, all the factors like ASA and AAF were largest in the semi-circular basin and least in the trapezoidal basin for the considered model parameters. The obtained largest AAF level near the edge of rectangular basin was also reported by Moczo and Bard (1993) and intense damage during past earthquakes (Poceski, 1969; Yuan and Huang, 1992).

On an average, an increase of ASA/AAF was obtained with an increase of IC, sediment quality factor and the basin shape-ratio (in the range 0.03 - 0.20). Furthermore, an increase of ground motion amplification towards the centre of basin with the decrease of sediment-damping reflects the effects of damping mainly on the basin-generated surface waves. The percentage increase of ground motion amplification is more than the percentage increase of IC across the basement. This may be due to the increased duration and trapping of surface waves in the basin due to an increase of IC. Based on the analysis of responses of basins for the different angles of incidence of SH-waves, it may be concluded that amplification of ground motion increases with the increase of angle of incidence of SH-waves in the basin. For example, the largest AAF was of the order of 1.63 and 1.69 for angle of incidence of 45^0 and 60^0, respectively.

ACKNOWLEDGMENTS

The research study presented in this paper has been carried out under the Dr. D.S. Kothari Postdoctoral Fellowship (DSKPDF) scheme. This study is financially supported by UGC research grant DSKPDF (F.4-2/2006(BSR)/ES/15-16/0037).The authors are grateful to an anonymous reviewer for objective evaluation and useful suggestions. They also express their thanks to Chief Editor of JIGU for apt editing.

Compliance with Ethical Standards

The authors declare that they have no conflict of Interest and adhere to copyright norms.

REFERENCES

Bard, P.Y., and Bouchon, M., 1980. "The seismic response of sediment-filled valleys. Part 1. The case of incident SH waves", Bull. Seism. Soc. Am., v.70, pp: 1263-1286.

Booth, D.B., Wells, R.E., and Givler R.W., 2004. "Chimney damage in the greater Seattle area from the Nisqually earthquake of 28 February 2001", Bull. Seis. Soc. Am., v.94, no.3, pp: 1143-1158.

Chavez-Garcia, F.J., and Faccioli, E., 2000. "Complex site effects and building codes: making the leap", Jr. Seismology, v.4, pp: 23-40.

Clayton, R.W., and Engquist, B., 1977. "Absorbing boundary conditions for acoustic and elastic wave equations", Bull. Seism. Soc. Am., v.67, pp: 1529-1540.

Dobry, R., and Vucetic, M., 1987. "State-of-the-Art Report: Dynamic Properties and Response of Soft Clay Deposits," Sociedad Mexicana de Mecanica de Suelos, v.2, pp: 51-87.

Emmerich, H., and Korn, M., 1987. "Incorporation of attenuation into time-domain computations of seismic wave fields", Geophysics, v.52, no.9, pp: 1252-1264.

Gao, S., Liu, H., Davis, P.M., and Knopoff, G.L., 1996. "Localized amplification of seismic waves and correlation with damage due to the Northridge earthquake", Bull. Seis. Soc. Am., v.86, no.1B, pp: S209-S230.

Graves, R.W., Pitarka, A., and Somerville, P.G., 1998. "Ground motion amplification in the Santa Monica area: Effects of shallow basin edge structure", Bull. Seism. Soc. Am., v.88, no.5, pp: 1224 -1242.

Hatyama, K., Matsumami, K., Iwata, T., and Irikuna, K., 1995. "Basin- induced love wave in the eastern part of the Osaka basin", Journal of Physics of the Earth, v.43, no.2, pp: 131- 155.

Israeli, M., and Orszag, S.A., 1981. "Approximation of Radiation Boundary Conditions", J. Comp. Phys., v.41, no.1, pp: 115-135.

Joshi, A., Kumar, P., Mohanty, M., Bansal, A.R., Dimri, V.P., and Chadha, R.K., 2012. "Determination of $Q_\beta(f)$ in different parts of Kumaon Himalaya from the inversion of spectral acceleration data", Pure and applied Geophysics, v.169, no.10, pp: 1821-1845.

Kamal, and Narayan, J.P., 2014. "3D basin-shape-ratio effects on frequency content and spectral amplitudes of basin-generated surface waves and associated spatial ground motion amplification and differential ground motion", Jr. Seismol DOI 10.1007/s10950-014-9466-8.

Kamal, and Narayan, J.P., 2015. "Study of effects of sediment-damping, impedance contrast and size of semi-spherical basin on the focusing and trapping of the basin-generated surface waves", Jr. of Earthquake Engineering, DOI: 10.1080/13632469.2015.1085461.

Kawase, H., 1996. "The cause of the damage belt in Kobe. 'the basin-edge effect', constructive interference of the direct S wave with the basin-induced diffracted/Rayleigh waves", Seismological Research Letters, v.67, no.5, pp: 25-35.

Kristeck, J., and Moczo, P., 2003. "Seismic wave propagation in viscoelastic media with material disconuties – a 3D 4th order staggered grid finite difference modeling", Bull. Seism. Soc. Am., v.93, no.5, pp: 2273-2280.

Kumar, P., Joshi, A., and Verma, O.P., 2013. "Attenuation tomography based on strong motion data: Case study of central Honshu region, Japan", Pure and applied Geophysics, v.170, no.12, pp: 2087-2106.

Kumar, P., Joshi, A., Sandeep and Kumar, A., 2014. "Three-dimensional attenuation structure in the region of Kumaon Himalaya, India based on inversion of strong motion data", Pure and applied Geophysics, v.172, no.2, pp: 333-358.

Kumar, P., Joshi, A., Sandeep, Kumar, A., and Chadha, R.K., 2015. "Detailed Attenuation Study of Shear Waves in the Kumaon Himalaya, India, Using the Inversion of Strong-Motion Data", Bul.l Seism. Soc. Am., v.105, no.4, pp: 1836-1851

Kumar, N., Kumar, P., Chauhan, V., and Hazarika, D., 2016. "Variable anelastic attenuation and site effect in estimating source parameters of various major earthquakes including Mw 7.8 Nepal and Mw 7.5 Hindu kush earthquake by using far-field strong-motion data", International Journal of Earth Sciences, DOI 10.1007/s00531-016-1432-y.

Kumar, S., and Narayan, J.P., 2008. "Implementation of absorbing boundary conditions in a 4th order accurate SH-wave staggered grid finite difference program with variable grid size", Acta Geophysica, v.56, pp: 1090-1108.

Moczo, P., and Bard, P.Y., 1993. "Wave-Diffraction, Amplification and Differential Motion near Strong Lateral Discontinuities", Bull. Seism. Soc. Am., v.83, pp: 85-106.

Narayan, J.P., Sharma, M.L., and Kumar, A., 2002. "A seismological report on the January 26, 2001 earthquake at Bhuj, India", Seismological Research Letters, v.73, no.3, pp: 343-355.

Narayan, J.P., 2005. "Study of Basin-edge effects on the ground motion characteristics using 2.5-D modeling", PAGEOPH, v.162, no.2, pp: 273-289.

Narayan, J.P., and Singh, S.P., 2006. "Effects of soil layering on the characteristics of basin-edge induced surface waves and differential ground motion", Jr. of Earthquake Engineering, v.10, no.4, pp: 595-614.

Narayan, J.P., and Kumar S., 2008. "A (2, 4) parsimonious staggered grid SH-wave FD algorithm with variable grid size and VGR–stress imagining technique", PAGEOPH, v.165, pp: 271-295.

Narayan, J.P., 2012. "Effects of P-wave and S-wave impedance contrast on the characteristics of basin transduced Rayleigh waves", Pure and Applied Geophys., v.169, no.4, pp: 693-709.

Narayan, J.P., and Kumar, V., 2013. "A fourth-order accurate finite-difference program for the simulation of SH-wave propagation in heterogeneous viscoelastic medium", Geofizika, v.30, no.2, pp: 173-189.

Narayan, J.P., and Kumar, V., 2014. "P-SV wave time-domain finite-difference algorithm with realistic damping and a combined study of effects of sediment rheology and basement focusing", Acta Geophysica, v.62, no.3, pp: 1214-1245.

Pitarka, A., Irikura, K., Iwata, T., and Sekiguchi, H., 1998. "Three-dimensional simulation of the near fault motion for the 1995 Hyogoken Nanbu (Kobe), Japan, earthquake", Bull. Seism. Soc. Am., v.88, pp: 428-440.

Poceski, A., 1969. "The ground effects of the Skopje July 26, 1963 earthquake", Bull. Seism. Soc. Am., v.59, pp: 1-2.

Semblat, J.F., Kham, M., Parara, E., Bard, P.Y., Pitilakis, K., Makra, K., and Raptakis, D., 2005. "Site effects: basin geometry vs soil layering", SDEE, v.25, no.7-10, pp: 529-538.

Yuan, Y.G., and Huang, S., 1992. "Damage distribution and estimation of ground motion in Shidian (China) basin", in Proc. Int. Symp. 'Effects of Surface Geology on Seismic Motion', , 25-27 March, Odawara, Japan, v.1, pp: 281-283.

Received on: 25.4.17; Revised on: 11.5.17; Re-Revised on: 27.7.17; Accepted on: 1.8.17